



Contents lists available at ScienceDirect

Bioorganic & Medicinal Chemistry Letters

journal homepage: www.elsevier.com/locate/bmcl

5-Amino-pyrazoles as potent and selective p38 α inhibitors

Jagabandhu Das^{*}, Robert V. Moquin, Alaric J. Dyckman, Tianle Li, Sidney Pitt, Rosemary Zhang, Ding Ren Shen, Kim W. McIntyre, Kathleen Gillooly, Arthur M. Doweiko, John A. Newitt, John S. Sack, Hongjian Zhang, Susan E. Kiefer, Kevin Kish, Murray McKinnon, Joel C. Barrish, John H. Dodd, Gary L. Schieven, Katerina Leftheris

Bristol-Myers Squibb Research and Development, PO Box 4000, Princeton, NJ 08543-4000, USA

ARTICLE INFO

Article history:

Received 10 August 2010

Revised 4 October 2010

Accepted 6 October 2010

Available online 13 October 2010

Keywords:

p38 Inhibitors
Amino-pyrazoles

ABSTRACT

The synthesis and structure–activity relationships (SAR) of p38 α MAP kinase inhibitors based on a 5-amino-pyrazole scaffold are described. These studies led to the identification of compound **2j** as a potent and selective inhibitor of p38 α MAP kinase with excellent cellular potency toward the inhibition of TNF α production. Compound **2j** was highly efficacious in vivo in inhibiting TNF α production in an acute murine model of TNF α production. X-ray co-crystallography of a 5-amino-pyrazole analog **2f** bound to unphosphorylated p38 α is also disclosed.

© 2010 Elsevier Ltd. All rights reserved.

Identification of potent and selective p38 α inhibitors as clinical candidates for the treatment of inflammatory disorders has been an area of continued interest in the pharmaceutical industry.¹ We recently disclosed a novel series of pyrazolo-pyrimidines as potent and selective inhibitors of the p38 α MAP kinase.² X-ray co-crystallographic studies of pyrazolo-pyrimidine **1** complexed with p38 α revealed some of the key binding interactions (Fig. 1). One of the pyrazole nitrogens is engaged in a H-bond interaction with the backbone of hinge residue Met109. The aniline group occupies the hydrophobic selectivity pocket while the aniline NH forms a H-bond with gate keeper Thr106 and the carboxamide NH with Glu71. Lack of any productive interaction of the pyrimidine ring with the enzyme suggested that the bicyclic core may be truncated to an amino-pyrazole core **2** which could maintain all the key H-bond interactions.

In this Letter we describe the synthesis and structure–activity relationship (SAR) studies in the 5-amino-pyrazole series **2** that led to the identification of compound **2j** as a potent and selective p38 α inhibitor. Analog **2j** was also highly efficacious in vivo in an acute pharmacodynamic model of TNF α production in mice.

The synthesis of amino-pyrazole analogs **2** with a primary amino substituent at C5 followed a general route as outlined in Scheme 1. Condensation of hydrazine **3** with 2-ethoxymethyl-malononitrile **4** in ethanol in the presence of triethylamine³ formed 5-aminopyrazole **5**. Saponification of **5** with aq sodium hydroxide in ethanol afforded carboxylic acid **6** which was coupled with aniline **7** under standard peptide coupling conditions (HATU, *i*-Pr₂NEt, DMF) to form **2**. Alternatively, the carboxylic acid **6** was

converted to its acid chloride which was subsequently treated with aniline **7** to afford **2** in excellent yield.^{4a}

The synthesis of amino-pyrazole analogs **2** with a secondary amino substituent at C5 followed a similar route (Scheme 2). Accordingly, alkylation of amino-pyrazole **6** with an alkyl bromide in THF in the presence of sodium hydride formed amino-pyrazole **8**. Alternatively, diazotization of **5** with *tert*-butyl nitrite in acetonitrile followed by addition of Cu(II) bromide formed a bromo derivative which is treated with an alkyl amine in ethanol at elevated temperature to form **8**. Saponification, followed by coupling of acid **9** with aniline **7** under similar conditions as described in Scheme 1 afforded analogs **2**.

The preliminary structure–activity optimization studies of the amino-pyrazoles (**2**) are outlined in Tables 1–3. Compounds were evaluated for their ability to inhibit phosphorylation of substrate (myelin basic protein) by recombinant human p38 α .^{4b} A peripheral blood mononuclear cell based assay (hPBMC) was used to measure the ability of compounds to inhibit LPS-induced TNF α production in human primary cells.⁸

Table 1 summarizes some of the key SAR findings for carboxamide modification with the *N*-1-phenyl-5-amino-pyrazole core. Both the methyl and ethyl amide analogs **2a** and **2b** were found to be equipotent to the pyrazolo-pyrimidine analog **1** in the p38 α enzyme and cellular assays. The corresponding cyclopropyl carboxamide **2c** also retained activity in both enzyme and cellular assays. A significant improvement in biochemical potency and more importantly, the cellular potency was observed with the *N*-methyl and *N*-ethyl-pyrazole analogs **2d**, and **2e**, respectively. Finally, the isoxazole amide **2f** was found to be one of the most potent inhibitor within this series.

^{*} Corresponding author. Tel.: +1 609 252 5068; fax: +1 609 252 6804.
E-mail address: jagabandhu.das@bms.com (J. Das).

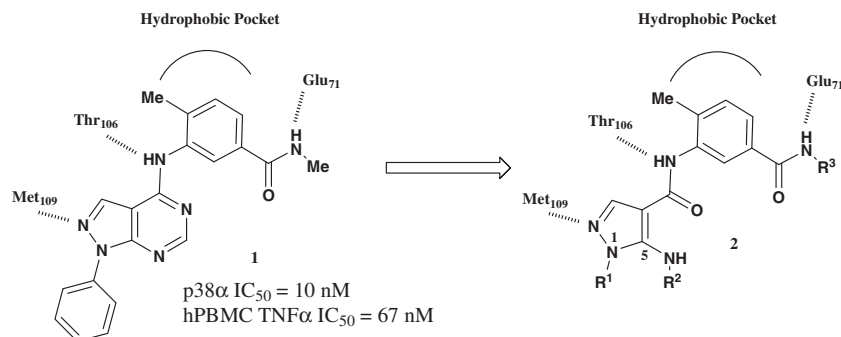


Figure 1. Binding mode of pyrazolo-pyrimidine **1** based on X-ray data. Proposed binding mode of amino-pyrazoles **2**.

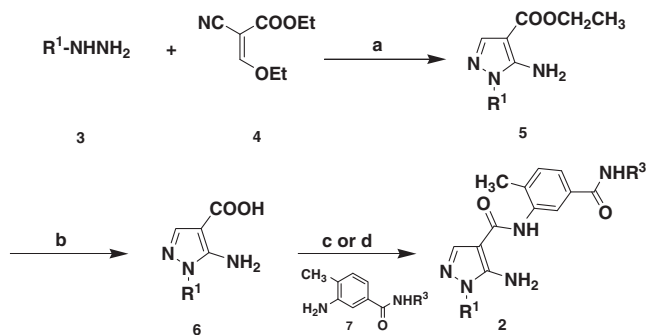
Based on the improved cellular potencies of the *N*-methyl-pyrazole (**2d**), *N*-ethyl-pyrazole (**2e**), and isoxazole carboxamides (**2f**), further SAR optimization was focused on these analogs. Some of the key SAR observations for N1 substitution are summarized in Table 2. Replacement of the phenyl group in isoxazole carboxamide **2f** with a pyridine ring (**2g**) retained the biochemical potency in vitro. However, analog **2g** is eightfold less potent than **2f** in the cellular assay. Substitution at either 2- or 4-position on the phenyl ring was well tolerated. The 2-*F*-phenyl derivative **2j** was identified to be the most potent analog in the cellular assay (TNFα IC₅₀ = 1 nM). Finally, N1 phenyl can be replaced with an alkyl group (**2m, n**) without significant loss in potency in both the biochemical and cellular assays.

We next proceeded to SAR studies focused on 5-amino substitution⁵ (Table 3). Alkylation of the 5-amino group showed some

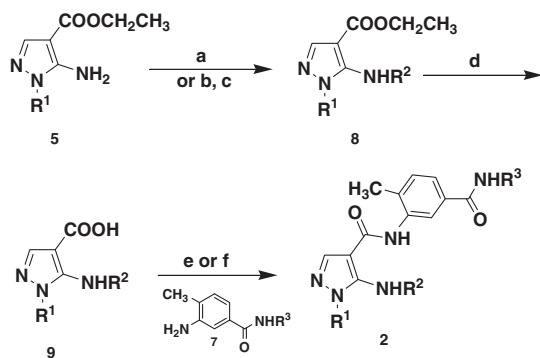
mixed results. The methylamine analog **2o** was less potent in the cellular assay despite retaining the biochemical activity relative to the amino derivative **2f**. A similar trend was observed with the 5-aminoethyl-N1-pyridyl analog **2q** compared to **2g**. In contrast, ethyl carboxamide analog **2p** retained both enzyme and cellular potencies of the corresponding 5-amino derivative **2b**. The 5-aminoethyl analog **2r** was identified as one of the most potent p38α inhibitors in this series.

Based on its both enzyme and cellular p38α inhibitory potencies, compound **2j** was selected for further evaluation. The kinase selectivity profile of **2j** was determined against several receptor, non-receptor tyrosine kinases, and serine/threonine kinases (Table 4). Compound **2j** was shown to be at least 2500-fold selective over these different kinases.

Compound **2j** was further profiled as a representative example of this novel chemotype (Table 5). In addition to its highly potent p38α inhibitory potencies in both biochemical and cellular assays, and exquisite selectivity over other kinases, compound **2j** was devoid of any significant Herg and CYP liability issues (low levels of



Scheme 1. Reagents and conditions: (a) EtOH, Et₃N, 60 °C, 1 h, 60%; (b) EtOH, aq NaOH; (c) HATU, *i*-Pr₂NEt, DMF; (d) SOCl₂, CH₂Cl₂; CH₂Cl₂, *i*-Pr₂NEt.



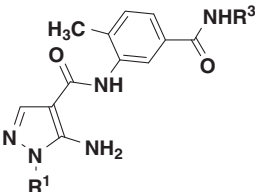
Scheme 2. Reagents and conditions: (a) NaH, THF, R²Br; (b) AcCN, *t*-BuONO, CuBr₂; (c) R²NH₂, EtOH, 150 °C; (d) EtOH, aq NaOH; (e) HATU, *i*-Pr₂NEt, DMF; (f) SOCl₂, CH₂Cl₂; CH₂Cl₂, *i*-Pr₂NEt.

Table 1
SAR for 4-carboxamide modification

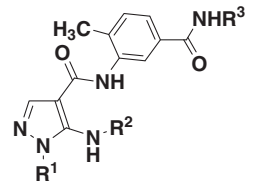
Compds	R ³	p38α IC ₅₀ , nM ^a	hPBMCTNFα IC ₅₀ , nM ^b
1	—	10	67
2a	Me	14	48
2b	Et	8	16
2c		7	26
2d		7	5
2e		5	8
2f		3	1

^a n = 4, variation in individual values, <20%.

^b n = 3, variation in individual values, <25%.

Table 2
SAR for N-1 substitution


Compds	R ¹	R ²	p38 α IC ₅₀ , nM ^a	hPBMC TNF α IC ₅₀ , nM ^b
2g	2-Pyridyl		2	8
2h	2-F-phenyl		3	5
2i	2-F-phenyl		4	2
2j	2-F-phenyl		2	1
2k	4-F-phenyl		2	2
2l	4-F-phenyl		2	2
2m	<i>n</i> -Bu		7	17
2n	<i>n</i> -Bu		2	2

^a *n* = 4, variation in individual values, <20%.^b *n* = 3, variation in individual values, <25%.**Table 3**
SAR for 5-amino substitution


Compds	R ¹	R ²	R ³	p38 α IC ₅₀ , nM ^a	hPBMC TNF α IC ₅₀ , nM ^b
2f	Ph	H		3	1
2o	Ph	Me		5	7
2p	Ph	Et		6	15
2q	2-Pyridyl	Et		4	30
2r	2-Me-phenyl	Et		5	1

^a *n* = 4, variation in individual values, <20%.^b *n* = 3, variation in individual values, <25%.

inhibitions). In addition, compound **2j** demonstrated excellent stability in rat, mouse, and human liver microsome assays⁶ in vitro. Compound **2j** also had good aqueous solubility at physiologic pH and excellent permeability as determined by Caco-2 cell perme-

Table 4
Kinase selectivity profile of **2j**

Kinase	IC ₅₀ (μM)	Kinase	IC ₅₀ (μM)
p38α	0.002	Lck	7
KDR	>50	Lckζ	>50
Btk	>15	VEGF	>50
CaMKII	>50	Tyk2	>5
MK2	>30	PLK1	>15
Itk	>50	DGAT	>20
STAT3	>10	PKAβ	>40
FGFR1	>50	PKCα	>40
GSK3	>5	PKCδ	>40
Syk	>50	PKCτ	>13
IGF-1R	>50	PKCζ	>20
Jak3	>10	PDGFβ	9.2

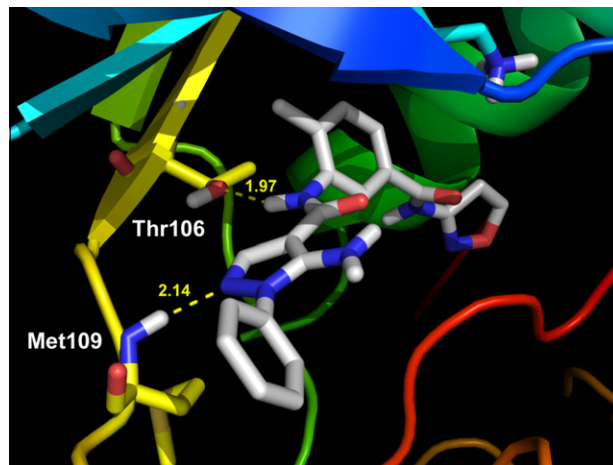
Table 5
In vitro profiling data for 5-amino-pyrazole analog **2j**

Parameter	Result
p38α IC ₆₀	1.97 nM
hPBMC LPS-TNFα IC ₅₀	1.2 nM
hERG ^a IC ₅₀	>160 μM
Metabolic stability ^b	HLM 0.001, RLM 0.000, MLM 0.000 ^c
CYP ^d inhibition IC ₅₀	> 40 μM 1A2, 2D6, 3A4; >13 μM 2C19; 23 μM 2C9
Aq Soln, pH 6.5	33 μg/mL
Caco-2 permeability	231 nm/s
Murine LPS-TNFα	>75% inhibition
Predose (5 mg/kg; 24 h)	

^a Flux assay.^b nmol/min/mg protein.^c HLM, human liver microsome; RLM, rat liver microsome; MLM, mouse liver microsome.^d CYP, cytochrome P450.

ability studies. The in vivo efficacy of **2j** was demonstrated in an acute pharmacodynamic model of LPS-induced TNF α production in mice. Mice were dosed orally with **2j** at 5 mg/kg, 24 h prior to LPS administration and the plasma TNF α level was measured 90 min later. Compound **2j** inhibited circulating TNF α level by >75%.⁴

To understand the binding mode of this novel class of p38 α inhibitors, compound **2f** was co-crystallized with purified, unphosphorylated p38 α MAP kinase and the X-ray structure of the complex determined.^{2,7,8} The key binding interactions between compound **2f** and the p38 α enzyme are illustrated in Figure 2.

**Figure 2.** Binding interactions between **2f** and unphosphorylated p38 α based on X-ray crystallographic analysis. Hydrogen bond distances are given in angstroms with key protein residues labeled.

The X-ray structure of **2f** reveals a combination of H-bonding and hydrophobic interactions. Consistent with our previous findings with other p38 α inhibitors, the pendant carboxamido-aniline ring occupies an angular hydrophobic pocket and makes key hydrogen bond interactions. Specifically, the aniline NH is H-bonded with Thr106 (1.97 Å). The hinge region residue, Met109 forms an H-bond with one of the pyrazole nitrogens (2.14 Å). The phenyl ring attached to the pyrazolo-pyrimidine ring is skewed out of plane. This orientation may explain some of the SAR observed regarding substitution at the *ortho*-position of the phenyl ring.

In conclusion, we utilized structure based drug design to identify a series of exquisitely potent and selective p38 α inhibitors using a novel 5-amino-pyrazole scaffold. SAR optimization at multiple positions led to the identification of analog **2j** as one of the most potent p38 α inhibitor with single digit nanomolar potency for inhibition of TNF- α release in human peripheral blood mononuclear cells (PBMCs). Oral efficacy was also demonstrated with this analog in an acute murine model of TNF α inhibition. In addition, the molecular basis for p38 α inhibition of this inhibitor class was established via X-ray crystal structure determination of an enzyme-inhibitor complex of a related analog **2f**.

References and notes

- For some recent reviews, see: (a) Sweeney, S. E. *Nat. Rev. Rheumatol.* **2009**, *5*, 475; (b) Schieven, G. L. *Curr. Top. Med. Chem.* **2005**, *5*, 921; (c) Saklatvala, J. *Curr. Opin. Pharm.* **2004**, *4*, 372; (d) Kumar, S.; Boehm, J.; Lee, J. C. *Nat. Rev. Drug Disc.* **2003**, *2*, 717; (e) Goldstein, D. M.; Kuglstatter, Y. L.; Soth, M. J. *J. Med. Chem.* **2009**, *53*, 2345; (f) Wagner, G.; Laufer, S. *Med. Res. Rev.* **2006**, *26*, 1; (g) Westra, J.; Limburg, P. C. *Mini-Rev. Med. Chem.* **2006**, *6*, 867.
- Das, J.; Moquin, R. V. M.; Pitt, S.; Zhang, R.; Shen, D. R.; McIntyre, K. W.; Gillooly, K.; Doweyko, A. M.; Sack, J. S.; Zhang, H.; Kiefer, S. E.; Kish, K.; McKinnon, M.; Barrish, J. C.; Dodd, J. H.; Schieven, G. L.; Leftheris, K. *Bioorg. Med. Chem. Lett.* **2008**, *18*, 2652.
- Schmidt, P.; Druey, J. *Helv. Chim. Acta* **1956**, *39*, 986.
- (a) For experimental details, see: Dyckman, A. J.; Das, J.; Leftheris, K.; Liu, C.; Moquin, R. V.; Wroblewski, S. U.S. Patent 7,390,810 B2, 2008; For a description of the biological assays, and X-ray crystal structure determination protocol, see: (b) Hynes, J., Jr.; Dyckman, A. J.; Lin, S.; Wroblewski, S. T.; Wu, H.; Gillooly, K. M.; Lonial, H.; Loo, D.; McIntyre, K. W.; Pitt, S.; Shen, D. R.; Shuster, D. J.; Zhang, X.; Behnia, K.; Marathe, P. H.; Doweyko, A.; Barrish, J.; Dodd, J.; Schieven, G.; Leftheris, K. *J. Med. Chem.* **2008**, *51*, 4.
- For additional 5-substitution SAR in this series, see: Dyckman, A. J.; Li, T.; Das, J.; Moquin, R. V. M.; Pitt, S.; Zhang, R.; Shen, D. R.; McKinnon, M.; McIntyre, K. W.; Gillooly, K.; Shuster, D.; Taylor, T.; Doweyko, A. M.; Sack, J. S.; Zhang, H.; Marathe, P.; Barrish, J. C.; Dodd, J. H.; Leftheris, K., manuscript in preparation.
- Rat, Mouse and Human Liver Microsome Stability Assays: Rat and mouse microsomes were purchased from XenoTech (Kansas City, KS). The human microsomes were purchased from In Vitro Technology (Baltimore, MD) and were pooled from 10 individual donors. The rates of oxidative metabolism were measured in triplicate under the following conditions: compound **2j**, 3 μ M final concentration; final microsomal protein concentration approximately 1 mg/mL; NADPH 1 mM; pH 7.4 potassium phosphate buffer, 56 mM. Incubations were performed at 37 °C and were initiated by the addition of the substrate. Aliquot (100 μ L) of the incubation were quenched at 0, and 10 min by the addition of 1 volume of acetonitrile. Results from 10-min incubations were used for the rate calculations. Sample were analyzed by the LC/MS/MS assay for the amount of the drug remaining at any time point. The percent metabolized was calculated based on the disappearance of the parent compound.
- Sack, J. S.; Kish, K. F.; Pokross, M.; Xie, D.; Duke, G. J.; Tredup, J. A.; Kiefer, S. A.; Newitt, J. A. *Acta Crystallogr., Sect. D* **2008**, *64*, 705.
- The X-ray coordinates have been deposited with the RCSB Protein Data Bank (RCSB ID Code: rcsb060940 and PDB ID Code: 3OCG).